VNU Journal of Science: Natural Sciences and Technology, Vol. 36, No. 3 (2020) 17-23

VNU Journal of Science: Natural Sciences and Technology

Journal homepage: https://js.vnu.edu.vn/NST

Original Article

Enhancement in Graphitization of Ordered Mesoporous Carbon by Assistance of Soybean Oil Surfactant

Le Thi Thu Hang*, Hoang Thi Bich Thuy

Hanoi University of Science and Technology, 1 Dai Co Viet, Hai Ba Trung, Hanoi, Vietnam

Received 05 February 2020
Revised 27 August 2020; Accepted 30 August 2020

Abstract: In this work, highly ordered mesoporous graphitic carbon (G-CMK3) has been prepared successfully by a nano-casting method using sucrose as carbon source, mesoporous silica as hard template, and soybean oil as surfactant. In the absence of soybean oil surfactant, the synthesized ordered mesoporous carbon material, CMK-3, revealed a low graphitization degree with a specific surface area of 1049.1 m^2/g and a high pore volume of 1.172 cm^3/g. However, with the assistance of soybean oil surfactant, the graphitization degree was improved significantly, which was confirmed by the decrease in the I_D/I_G intensity ratio of the D (disordered or amorphous structure) and G (graphitic structure) peaks from 0.98 to 0.83. After the synthesis in the presence of soybean oil, G-CMK3 carbon maintained the integrity of the mesoporous structure albeit with a slight decrease in its specific surface area (845.2 m^2/g) as well as pore volume (0.858 cm^3/g).

Keywords: Mesoporous carbon, hard templates, nanorods, graphitic carbon, soybean oil.

1. Introduction

Carbon materials have widely used in many applications such as gas separation, water purification, catalyst supports, catalyst, energy storage and conversion [1]. Currently, numerous carbon material types, for example, carbon nanotubes (CNTs), graphene, mesoporous carbon, carbon nanofiber, carbon microfibers, have been prepared and investigated [2]. Among them, ordered mesoporous carbon (OMC) materials have gained a great attention because of their excellent textural characteristics and mesoporous network. They provide a highly opened 3D porous host with easy access for guest species, thus facilitating diffusion throughout the pore channels without pore blockage. Especially, because of these superior features, OMC materials have been recognized to be promising active electrode materials or

* Corresponding author.
Email address: hang.lethithu@hust.edu.vn

https://doi.org/10.25073/2588-1140/vnunst.4989

electrode scaffolds for supercapacitors, and rechargeable batteries in the field of energy storage and conversion.

The OMC materials are frequently prepared by two methods including *(i)* self-assembly using soft templates through co-condensation and carbonization, and *(ii)* replication synthesis with pre-synthesized hard templates through impregnation, carbonization, and template removal. Two methods are referred to the soft template and hard template methods, respectively [3]. Each of these methods has different advantages and disadvantages. For the soft template method, the mesoporous carbon structure is formed by self-assembly of organic molecules. Thus, elimination of soft templates in the synthesis process of OMC materials is generally easy and convenient. However, the soft template synthesis exhibits a disadvantage of wide pore-size distribution with irregular pore shape. In contrast, the hard template synthesis enables better controlling the pore size and shape of the obtained OMC [4-7]. Nevertheless, hard templates removal is needed for this method to obtain the mesoporous structure.

Regardless of synthetic methods, electrochemical performance of the OMC material mainly depends on their capability to interact with ions and to transport electrons. For instance, for supercapacitor applications, OMC materials require high conductivity for electron transport, the high surface area for effective ion adsorption/desorption, and suitable pore architecture for rapid access of ions from the electrolyte to the electrode surface [8,9]. Generally, the electronic conductivity of carbon materials is strongly impacted by their graphitization degree [10]. Therefore, to improve the electrochemical performance of the OMC materials for energy storage and conversion applications, enhancement of the graphitization degree is essential.

In our previous reports, we successfully synthesized OMC from pure chemicals and/or natural kaolin clay sources [9,11,12]. The resultant OMC materials all showed the high application potential in lithium ion batteries and supercapacitors. With the aim of improving further the electrical conductivity for the OMC, in the present work, we suppose a facile synthetic strategy to enhance the graphitization degree for OMC materials. Thanks to the use of a cheap natural product, soybean oil, as surfactant, the formation of the graphitic framework structure of carbon are favorable. Accordingly, the electronic conductivity of the synthesized OMC materials can be improved significantly.

2. Materials and Methods

2.1. Preparation of OMC Materials

Highly graphitic ordered mesoporous carbon (denoted as G-CMK3) with the assistance of soybean oil were prepared by a nano-casting route using SBA-15 silica as hard template, sucrose as carbon source. SBA-15 silica was prepared via the process as previously reported [13]. The synthesis process is shown in Figure 1. In specific, 5 g of sucrose and 0.56 g of H_2SO_4 were solved into 20 mL of distilled water. Subsequently, 4 g of SBA-15 was added and dispersed for 30 minutes in an ultrasonic bath. Next, the mixture was dried at 100°C for 6 h and at 160°C for 12 h more to obtain a dark brown sample. After being ground by an agate mortar,

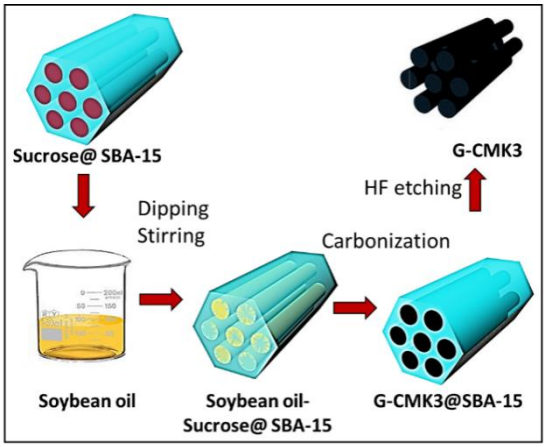

Figure 1. Schematic diagram of the synthetic process of G-CMK3.

and a pestle, the dark brown powder was re-dispersed in 15 mL of another aqueous solution of sucrose (3.2 g), and H_2SO_4 (0.36 g). After that, the sample was continuously dried at 160 °C for 12 h to generate the sucrose@SBA-15 composite, which was subsequently re-ground and dispersed into an excess amount of soybean oil under vigorous stirring for 6 h. After filtration, the soybean oil-sucrose@SBA-15 sample was carbonized in an inert gas at 900 °C for 5 h to produce G-CMK3@SBA-15. Finally, G-CMK3 was collected after etching SBA-15 template in 5 wt.% HF acid, washed thoroughly and dried at 100 °C in a vacuum oven overnight. For comparison, another sample was also prepared in the absence of soybean oil surfactant. This sample was referred to CMK3.

2.2. Microstructure and Physicochemical Characterizations

The microstructures of the materials were examined using a field emission scanning electron microscope (FESEM, S-4700/EX-200, Hitachi, Japan) equipped with an energy dispersive X-ray (EDX) detector, a high-resolution transmission electron microscope (HRTEM, Tecnai G2, Philips, the Netherlands), a high-resolution X-ray diffractometer (XRD, D/MAX Ultima III, Rigaku, Japan), and Raman spectrometer (Horiba Jobin-Yvon). Thermal stability of the materials was evaluated using a thermogravimetric analyzer (TGA, TGA-50, Shimadzu, Japan). The nitrogen adsorption-desorption isotherms were conducted on Brunauer-Emmett-Teller (BET) analysis system (ASAP 2020, Micromeritics, USA).

3. Results and Discussion

The morphologies of the synthesized materials were examined using SEM as shown in Figure 2. Figure 2c-f show the surface morphologies of both CMK3 and G-CMK3, which were totally analogous to the morphology of the SBA-15 hard template (Figure 2a,b). This implies that the morphology of the template was remained in CMK3 and G-CMK3 after template removal. The resultant carbon samples were comprised of uniform short nanorods. Each nanorod had a length of ~1μm and a diameter of ~400 nm. Noticeably, the nanorod size of the obtained carbon samples appeared smaller in comparison with the SBA-15 template. It is due to the shrinkage of carbon sources, viz. Sucrose, and soybean oil, which were used to fill into the SBA-15 template, during the carbonization process. From the high-resolution SEM images of CMK3 and G-CMK3, it is recognized that, as for G-CMK3 carbon in the presence of the soybean oil surfactant the surface of the nanorods seems to be smoother. In contrast, the nanorod surface of CMK3 looks rough with plenty of nanosized pores. This is ascribed to the lower carbon content, which was filled into the SBA-15 template, as illustrated in Figure 3a.

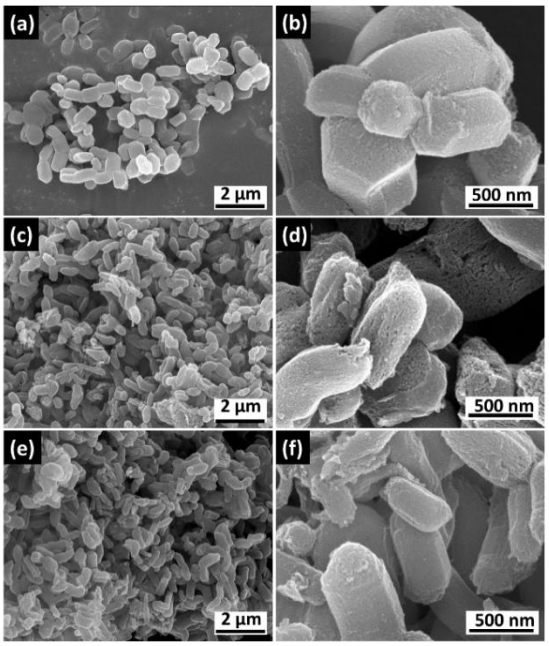

Figure 2. Low and high resolution SEM images of (a,b) SBA-15, (c,d) CMK3, and (e,f) G-CMK3.

Figure 3a presents the TGA plots of the CMK3@SBA-15 and G-CMK3@SBA-15 composites in the air. After sintering up to 800 °C in the air atmosphere, the carbon component of the mixtures burned out, and only SBA-15 silica was retained. According to the TGA results, the mass losses of 38.27 wt.% and 50.36

wt.% correspond to the carbon contents present the CMK3@SBA-15 and G-CMK3@SBA-15 composites, respectively. The carbon contribution of soybean oil into G-CMK3 was calculated to be 12.09 wt.%. This is indicative of the inclusion of soybean oil, which would play a role as an assistant promoting the graphitization of G-CMK3 carbon, into the sucrose@SBA-15 composite in the synthesis process.

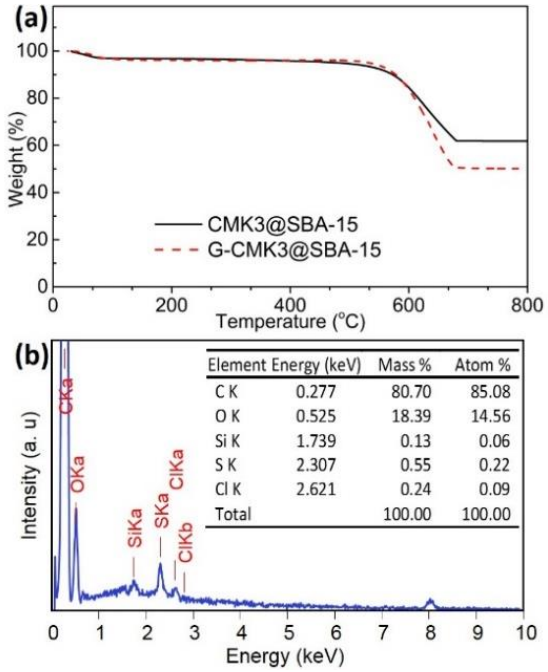

Figure 3. (a) TGA plots of CMK3@SBA-15 and G- CMK3@SBA-15. The heating rate of TGA measurements was 10 °C/min. (b) The EDX spectrum and composition table of G-CMK3.

In addition, to determine the purity of the synthesized carbon, EDX analysis was performed. Figure 3b depicts the typical EDX analysis result of G-CMK3. It is recognized that, apart from the main element, C, other elements such as O, Si, S, Cl were also detected. The C content was 80.70 wt.% while the Si content was only 0.13 wt.% (inset in Figure 3b). This demonstrates that SBA-15 template was removed completely from the G-CMK3@SBA-15 sample after the etching step (Figure 1). Herein, the presence of O element is attributed to the surface functionalization of carbon during the synthesis process and/or the adsorption of oxygen on the sample surface [14] Meanwhile, the presence of S and Cl is resulted from the chemicals used to synthesize the material. Similarly, the C, O, and Si contents of the CMK3 sample were measured to be 79.58, 19.11, and 0.41 wt.%, respectively, implying the high purity of the obtained CMK3 and G-CMK3.

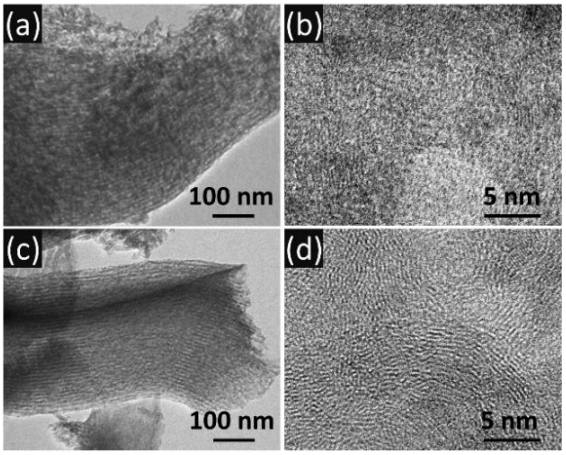

Figure 4. Low and high resolution TEM images of (a,b) CMK3 and (c,d) G-CMK3.

To investigate the textural structure of the obtained G-CMK3 material, the TEM method was employed. From Figure 4, it can be seen that both CMK3 and G-CMK3 possess the linear arrays of mesochannels arranged in a particular order. Compared with CMK3 carbon (Figure 4a), G-CMK3 carbon reveals a well organized mesoporous structure (Figure 4c). Regarding the high-resolution TEM images in Figure 4b,d, it can be claimed that the stacks of graphite layers are observed for both samples. This is evidence for the appearance of partially-graphitized carbon frameworks. However, a considerable number of defects was found for the CMK3 carbon without the assistance of soybean oil. Meanwhile, the more ordered and regular arrangement was easily recognized for G-CMK3 carbon. This demonstrates the benefit of the inclusion of soybean oil assistant in enhancing the graphitic degree of G-CMK3, during the synthesis process.

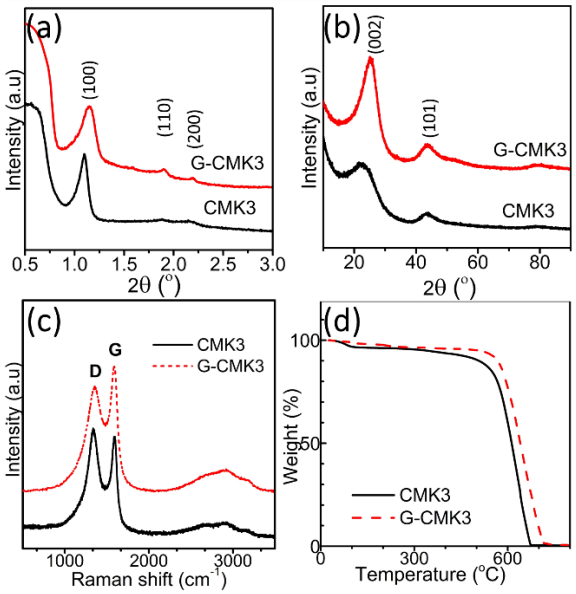

Figure 5. (a) Low angle and (b) wide angle XRD patterns, (c) Raman spectra, and (d) TGA plots of CMK3 and G-CMK3. The heating rate of TGA measurements was 10 °C/min.

To examine further the ordered structure of the synthesized G-CMK3 carbon, a low angle XRD measurement was carried out between 0.5° and 3.0°. As shown in Figure 5a, three sharp diffraction peaks of G-CMK3 were detected. Among them, the strongest peak located at 1.16° corresponding to the (100) plane of a two-dimensional hexagonal lattice structure of SBA-15 template. Whilst two remaining peaks represent the (110) and (200) planes [15]. This result implies the highly ordered structure of the resultant G-CMK3. Similarly, for CMK3 carbon without the assistance of soybean oil, the reflection intensities of the (110) and (200) planes were found to be relatively weak compared with G-CMK3 carbon, demonstrating a less ordered arrangement. This suggests that the presence of soybean oil promoted the orientation of carbon clusters along (110) and (200) directions of the hexagonal structure of SBA-15 template. On the other hand, the phase structures of CMK3 and G-CMK3 were determined by wide angle XRD measurements as shown in Figure 5b. Generally, the XRD patterns of both samples exhibit two peaks at 2θ = 24° and 2θ = 44°, corresponding to the (002) and (101) diffraction indexes of graphitized carbon, respectively. This indicates the nature of the turbostratic carbon structure of CMK3 and G-CMK3. This result in the present work is also in high agreement with the previous reports [16,17]. Remarkably, with the assistance of soybean oil, the diffraction peaks of G-CMK3 appear much sharper than that of CMK3 carbon, especially for the peak of the (002) plane.

Haman is well known as a powerful tool for the structural analyses of materials. Thus, to identify further the carbon structure, the Raman spectra of CMK3 and G-CMK3 were recorded. Figure 5c depicts Raman spectra of G-CMK3 and CMK3 carbon between 400 and 4000 cm^{-1}. As seen, characteristic bands for amorphous (D band, around 1350 cm^{-1}), and graphitic carbon materials (G band, around 1580 cm^{-1}) were detected for both two carbon samples. It is established that the degree of graphitization of carbon materials is generally evaluated by the intensity ratio of the D to G peaks (I_D/I_G) [18]. According to the analysis result of Figure 5c, the I_D/I_G ratios of the CMK3 and G-CMK3 samples were 0.98 and 0.83, respectively. This suggests that the amorphous feature of the CMK3 material dominates over that of the G-CMK3. In other words, G-CMK3 carbon with the assistance of soybean oil possessed the higher degree of graphitization than CMK3 carbon.

Furthermore, the higher graphitization degree of G-CMK3 was also verified by the TGA result. As seen in Figure 5d, it is obvious that, G-CMK3 showed the higher thermal stability than that of CMK3. In specific, in the air atmosphere, the G-CMK3 carbon started to decompose thermally at the temperature of 464°C. Meanwhile, the onset decomposition temperature of the CMK3 carbon was 311°C. The temperatures, at which the thermal decomposition process occurred strongly for G-CMK3 and CMK3, were found to be 573 and 559°C, respectively. Hence, it can be concluded that, in comparison with the CMK3 carbon, the G-CMK3 carbon synthesized with the assistance of soybean oil surfactant exhibited the higher

graphitization degree, which results in the higher thermal stability.

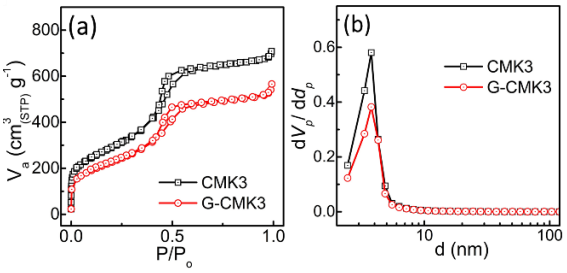

Figure 6. (a) Nitrogen adsorption-desorption isotherms and (b) relevant pore size distribution curves of CMK3 and G-CMK3.

Table 1. Textual parameters results from nitrogen adsorption and desorption isotherms of CMK-3 and G-CMK3 carbon.

Parameters	CMK3	G-CMK3
S_{BET} (m^2/g)	1049.1	845.2
Mean pore size (nm)	4.422	4.094
Pore volume (cm^3/g)	1.172	0.858

To clarify the mesoporous structure of synthesized G-CMK3 carbon, the sample was measured nitrogen adsorption-desorption isotherm at 77 K. For comparison, the CMK3 sample was measured as well. Figure 6a display nitrogen adsorption-desorption isotherms of CMK3 and G-CMK3. It is worth noting that characteristic hysteresis loops for mesoporous structure materials are observed for both samples. This evidences that CMK3 and G-CMK3 materials possessed mesosized pores. The specific surface area (SBET) of CMK3 was measured to be 1049.1 m^2/g while the specific surface area of G-CMK3 was only 845.2 m^2/g. This is explained by the deep penetration of the carbon precursors into the pores of SBA-15 template for G-CMK3. This led to the thicker wall of carbon nanopipes in the nanorod structure of G-CMK3. This is also the reason to explain why the pore volume and the mean pore size of G-CMK3 were smaller than those of CMK3 (Table 1). However, the decrease of the textual parameters of G-CMK3 are negligible.

4. Conclusion

Highly graphitic ordered mesoporous carbon G-CMK3 material has been synthesized successfully by "surfactant-assisted" nanocasting route with SBA-15 silica as template, sucrose as carbon source and soybean oil as surfactant as well as carbon source. The synthesized G-CMK3 exhibited a high specific surface area (845.2 m^2/g), and high porosity (0.858 m^3/g). Inclusion of soybean oil with sucrose into SBA-15 in the nanocasting step of the synthesis process was demonstrated to benefit enhancing the degree of graphitization for G-CMK3 carbon material while the textual parameters involving the specific surface area, mean pore size and volume pore were still comparable to that of CMK3 without the assistance of soybean oil. The use of natural soybean oil as environmentally friendly and cheap surfactant in the improvement of the degree of graphitization for carbon can be considered as an innovative point in the synthetic route of the ordered mesoporous graphitic carbon. Owing to the enhanced graphitization degree, the electronic conductivity of G-CMK3 will firmly be improved, following by huge promising applications, especially for electrochemical energy storage systems.

Acknowledgments

This research is funded by Vietnam National Foundation for Science and Technology Development (NAFOSTED) under grant number 104.99-2017.305.

References

[1] J. Lee, J. Kim, T. Hyeon, Recent Progress in the Synthesis of Porous Carbon Materials, Adv. Mater., 18 (2006) 2073-2094. https://doi.org/10.1002/adma.200501576.

[2] Z. Ma, X. Yuan, L. Li, Z.-F. Ma, D.P. Wilkinson, L. Zhang, J. Zhang, A review of cathode materials and structures for rechargeable lithium–air batteries, Energy Environ. Sci., 8 (2015) 2144-2198. https://doi.org/10.1039/C5EE00838G.

[3] W. Shou, R. Guo, H. Pan, D.D. Gang, Ordered Mesoporous Carbon: Fabrication, Characterization, and Application as Adsorbents, Dekker Encyclopedia of Nanoscience and Nanotechnology, CRC Press 2014, 4200. https://doi.org/10.1081/E-ENN3-120053279.

[4] M. Marcos-Hernández, D. Villagrán, 11 - Mesoporous Composite Nanomaterials for Dye Removal and Other Applications, G.Z. Kyzas, A.C. Mitropoulos (Eds.) Composite Nanoadsorbents, Elsevier 2019, pp.265-293. https://doi.org/10.1016/B978-0-12-814132-8.00012-5.

[5] N.T. Thao, Synthesis and characterization of carbon molecular sieve CMK-3 VNU Journal of Science, Natural Sciences and Technology, 27 (2011) 259-263.

[6] N.T. Thao, N.T.B. Ngoc. Comparative mesoporous carbon materials templated by SBA-15 synthesized from different silicate sources, Vietnam Journal of Chemistry, 51 (2013) 352-357.

[7] H.T.K.T. Hoa T. H. Nguyen, P. T. Dang, Synthesis of mesoporous carbon material by hard template method: a comparative study of SBA15 and MCF as templates, Vietnam Journal of Catalysis and Adsorption, 7 (2018) 83-88.

[8] J.W.F. To, Z. Chen, H. Yao, J. He, K. Kim, H.-H. Chou, L. Pan, J. Wilcox, Y. Cui, Z. Bao, Ultrahigh Surface Area Three-Dimensional Porous Graphitic Carbon from Conjugated Polymeric Molecular Framework, ACS Cent. Sci., 1 (2015) 68-76. https://doi.org/10.1021/acscentsci.5b00149.

[9] B.T.T. Huyen, L.T.T. Hang, Synthesis, Characteristics of CMK-3 Carbon Materials Derived on Various SBA-15 Templates and their Application in Electrochemical Supercapacitors, The Journal of Science & Technology of Technical Universities, 141 (2020) 051-056. (in Vietnamese).

[10] Y. Weni, Muldarisnur, The Effect of Graphitization Temperature on the Composition and the Electrical Conductivity of Carbon Nanotube, KnE Engineering, 1 (2019) 323-328.

[11] H.T.T. Le, T.-D. Dang, N.T.H. Chu, C.-J. Park, Synthesis of nitrogen-doped ordered mesoporous carbon with enhanced lithium storage performance from natural kaolin clay, Electrochim. Acta, 332 (2020) 135399.https://doi.org/ 10.1016/j.electacta.2019.135399.

[12] N.T.H. Chu, Q.L.D. Ngo, H.T.T. Le, Synthesis of Ordered Mesoporous Carbon from Vietnam Natural Kaolin Clay for Supercapacitor Application, Materials Science Forum, 985 (2020) 124–136. https://doi.org/10.4028/www.scientific.net/MSF.985.124.

[13] X. Ji, K.T. Lee, L.F. Nazar, A highly ordered nanostructured carbon–sulphur cathode for lithium–sulphur batteries, Nat. Mater., 8 (2009) 500-506. https://doi.org/10.1038/nmat2460.

[14] S. Andreoli, P. Benito, M.V. Solmi, G. Fornasari, A. Villa, B. Wu, S. Albonetti, Insights into the Synthesis and Surface Functionalization of Mesoporous Carbon for Catalytic Applications, ChemistrySelect, 2 (2017) 7590-7596. https://doi.org/10.1002/slct.201700924.

[15] M. Kruk, M. Jaroniec, C.H. Ko, R. Ryoo, Characterization of the Porous Structure of SBA-15, Chem. Mater., 12 (2000) 1961-1968. https://doi.org/10.1021/cm000164e.

[16] Z.Q. Li, C.J. Lu, Z.P. Xia, Y. Zhou, Z. Luo, X-ray diffraction patterns of graphite and turbostratic carbon, Carbon, 45 (2007) 1686-1695. https://doi.org/10.1016/j.carbon.2007.03.038.

[17] Y. Wang, X. Bai, F. Wang, H. Qin, C. Yin, S. Kang, X. Li, Y. Zuo, L. Cui, Surfactant-assisted Nanocasting Route for Synthesis of Highly Ordered Mesoporous Graphitic Carbon and Its Application in CO_2 Adsorption, Sci. Rep., 6 (2016) 26673. https://doi.org/10.1038/srep26673.

[18] X. Chen, X. Deng, N.Y. Kim, Y. Wang, Y. Huang, L. Peng, M. Huang, X. Zhang, X. Chen, D. Luo, B. Wang, X. Wu, Y. Ma, Z. Lee, R.S. Ruoff, Graphitization of graphene oxide films under pressure, Carbon, 132 (2018) 294-303. https://doi.org/10.1016/j.carbon.2018.02.049.